



Lecture 13. Temperature Lidar (2)

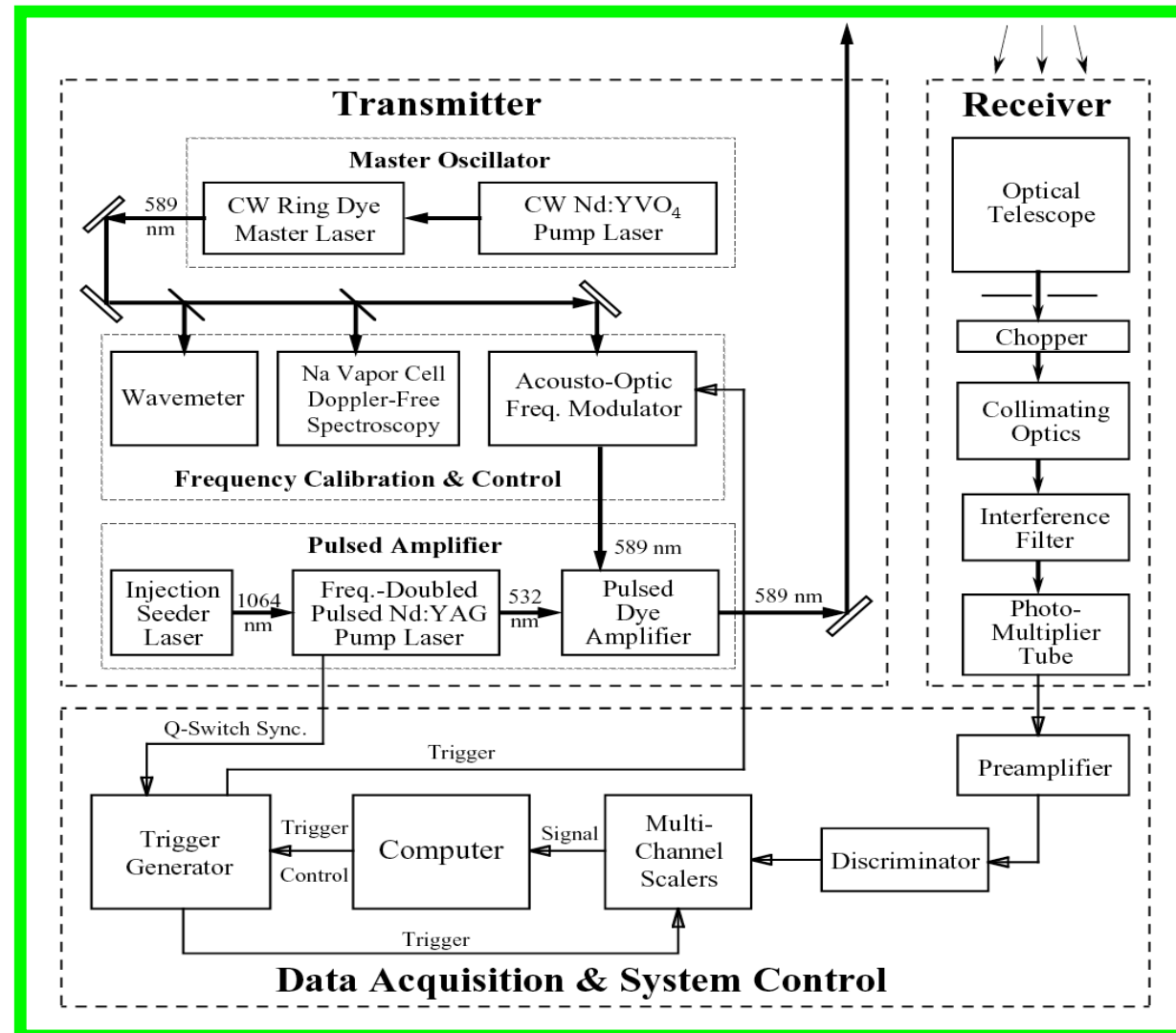
Resonance Fluorescence Doppler Tech

- ❑ Resonance Fluorescence Na Doppler Lidar
- Na Structure and Spectroscopy
- Scanning versus Ratio Techniques
- ❑ Principle of Doppler ratio technique
- Three-frequency ratio technique
- Comparison of calibration curves
- ❑ Other resonance fluorescence Doppler lidars
- K Doppler Lidar
- Fe Doppler Lidar
- ❑ Summary



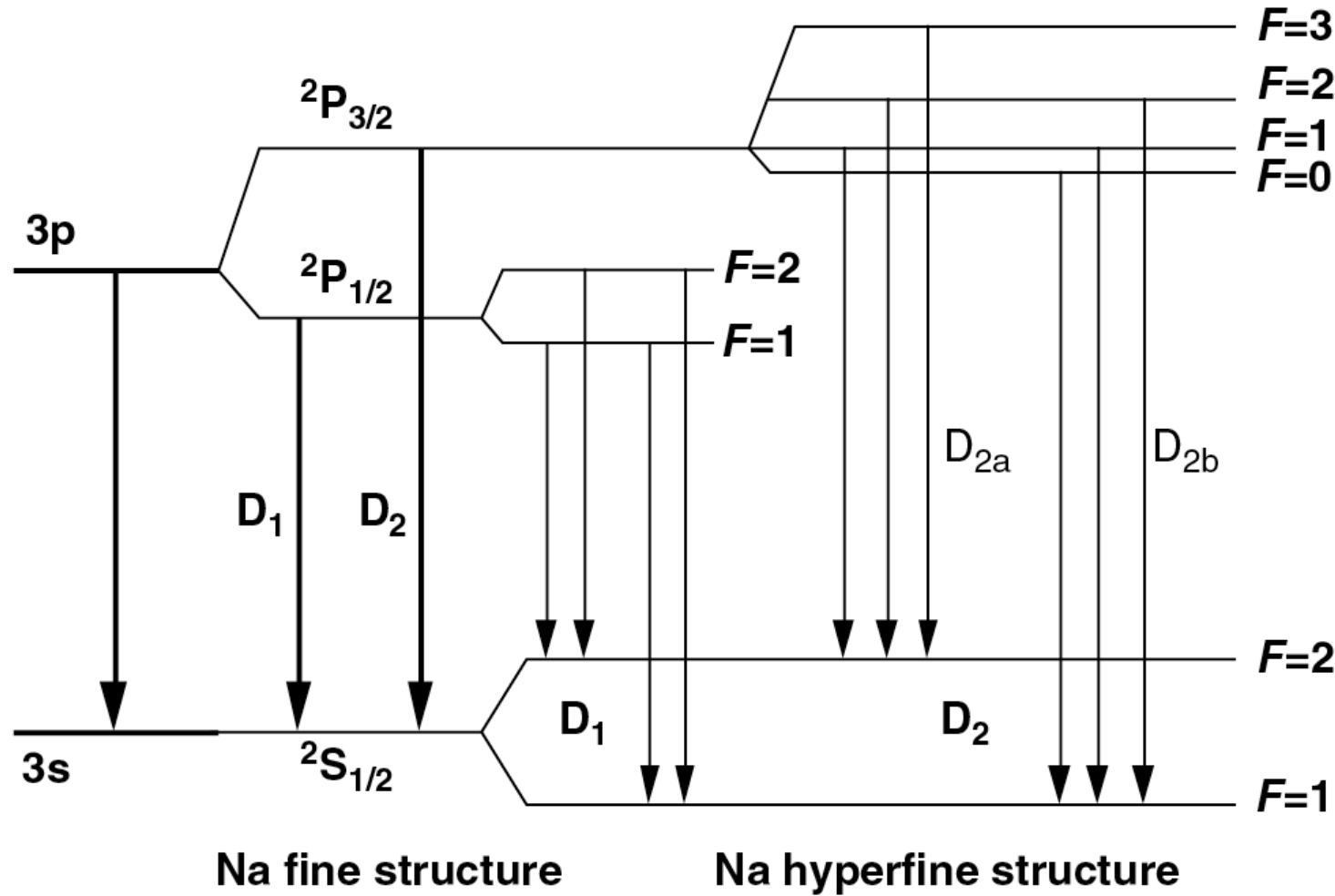
Na Doppler Wind and Temperature Lidar

- ❑ Na Doppler lidar is one of the most successful lidars.



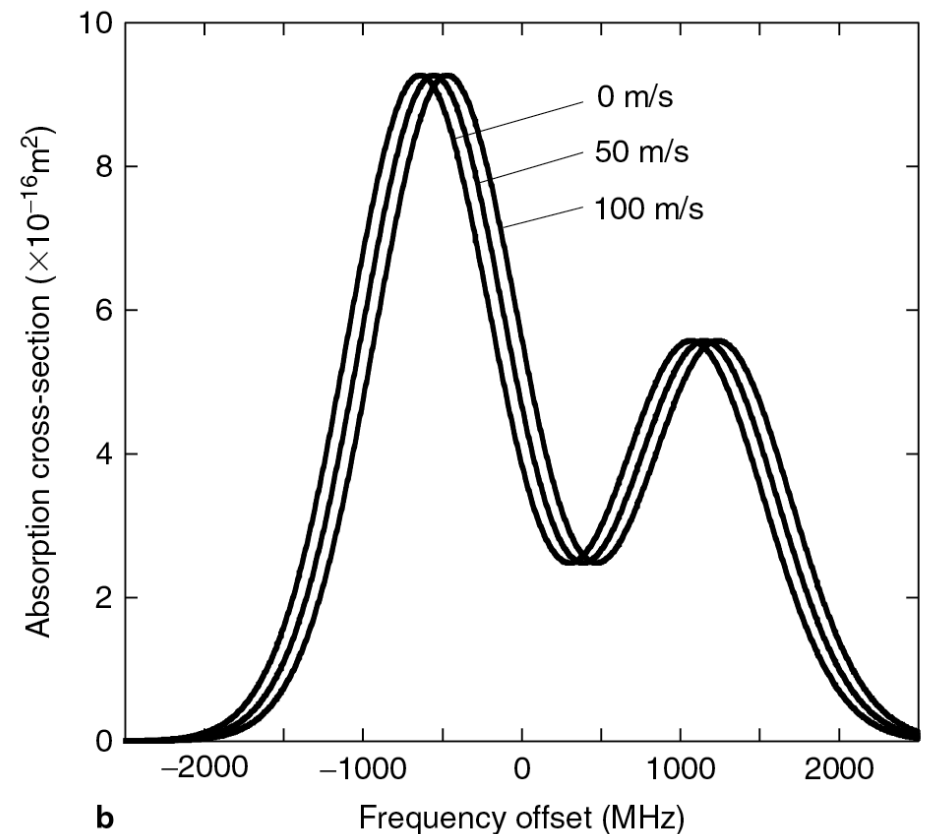
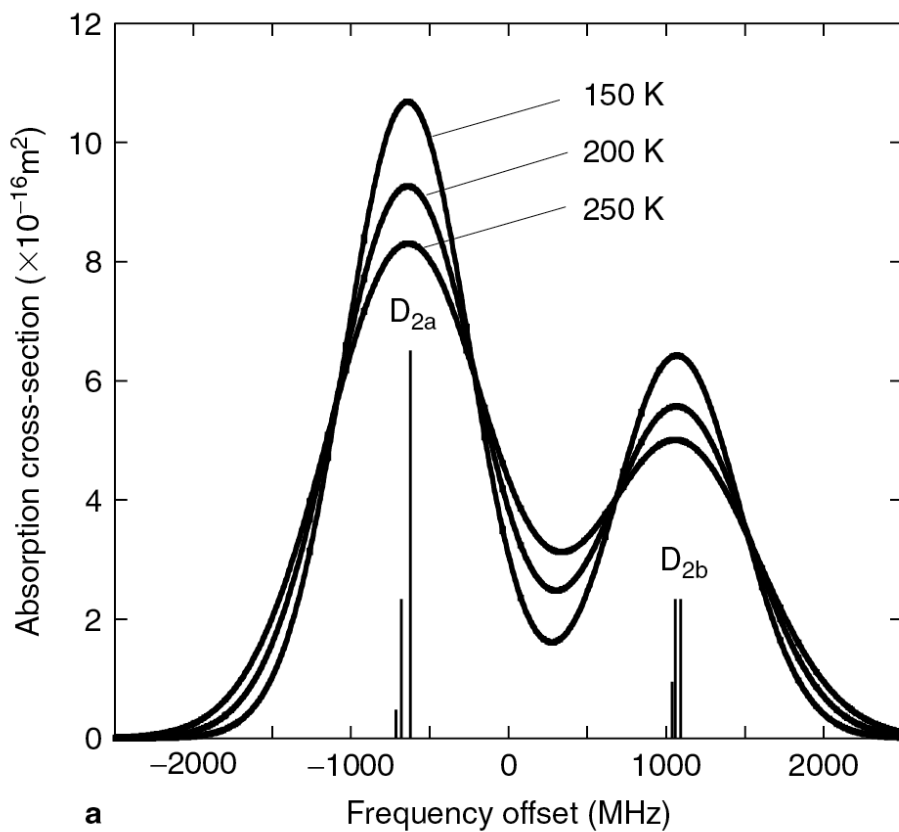


Na Atomic Energy Levels





Doppler Effect in Na D₂ Line Resonance Fluorescence



Na D₂ absorption linewidth
is temperature dependent

Na D₂ absorption peak freq
is wind dependent



Na Atomic Parameters

Table 5.1 Parameters of the Na D₁ and D₂ Transition Lines

Transition Line	Central Wavelength (nm)	Transition Probability (10^8 s^{-1})	Radiative Lifetime (nsec)	Oscillator Strength f_{ik}
D ₁ (${}^2\text{P}_{1/2} \rightarrow {}^2\text{S}_{1/2}$)	589.7558	0.614	16.29	0.320
D ₂ (${}^2\text{P}_{3/2} \rightarrow {}^2\text{S}_{1/2}$)	589.1583	0.616	16.23	0.641
Group	${}^2\text{S}_{1/2}$	${}^2\text{P}_{3/2}$	Offset (GHz)	Relative Line Strength ^a
D _{2b}	$F=1$	$F=2$	1.0911	5/32
		$F=1$	1.0566	5/32
		$F=0$	1.0408	2/32
D _{2a}	$F=2$	$F=3$	-0.6216	14/32
		$F=2$	-0.6806	5/32
		$F=1$	-0.7150	1/32

Doppler-Free Saturation–Absorption Features of the Na D₂ Line

f_a (MHz)	f_c (MHz)	f_b (MHz)	f_+ (MHz)	f_- (MHz)
-651.4	187.8	1067.8	-21.4	-1281.4

^aRelative line strengths are in the absence of a magnetic field or the spatial average. When Hanle effect is considered in the atmosphere, the relative line strengths will be modified depending on the geomagnetic field and the laser polarization.



Doppler-Limited Na Spectroscopy

- Doppler-broadened Na absorption cross-section is approximated as a Gaussian with rms width σ_D

$$\sigma_{abs}(\nu) = \frac{1}{\sqrt{2\pi}\sigma_D} \frac{e^2 f}{4\epsilon_0 m_e c} \sum_{n=1}^6 A_n \exp\left(-\frac{[\nu_n - \nu(1 - V_R/c)]^2}{2\sigma_D^2}\right) \quad (13.1)$$

- Assume the laser lineshape is a Gaussian with rms width σ_L
- The effective cross-section is the convolution of the atomic absorption cross-section and the laser lineshape

$$\sigma_{eff}(\nu) = \frac{1}{\sqrt{2\pi}\sigma_e} \frac{e^2 f}{4\epsilon_0 m_e c} \sum_{n=1}^6 A_n \exp\left(-\frac{[\nu_n - \nu(1 - V_R/c)]^2}{2\sigma_e^2}\right) \quad (13.2)$$

where (13.3) $\sigma_e = \sqrt{\sigma_D^2 + \sigma_L^2}$ and $\sigma_D = \sqrt{\frac{k_B T}{M \lambda_0^2}}$ (13.4)

The frequency discriminator/analyzer is in the atmosphere!



Doppler Scanning Technique

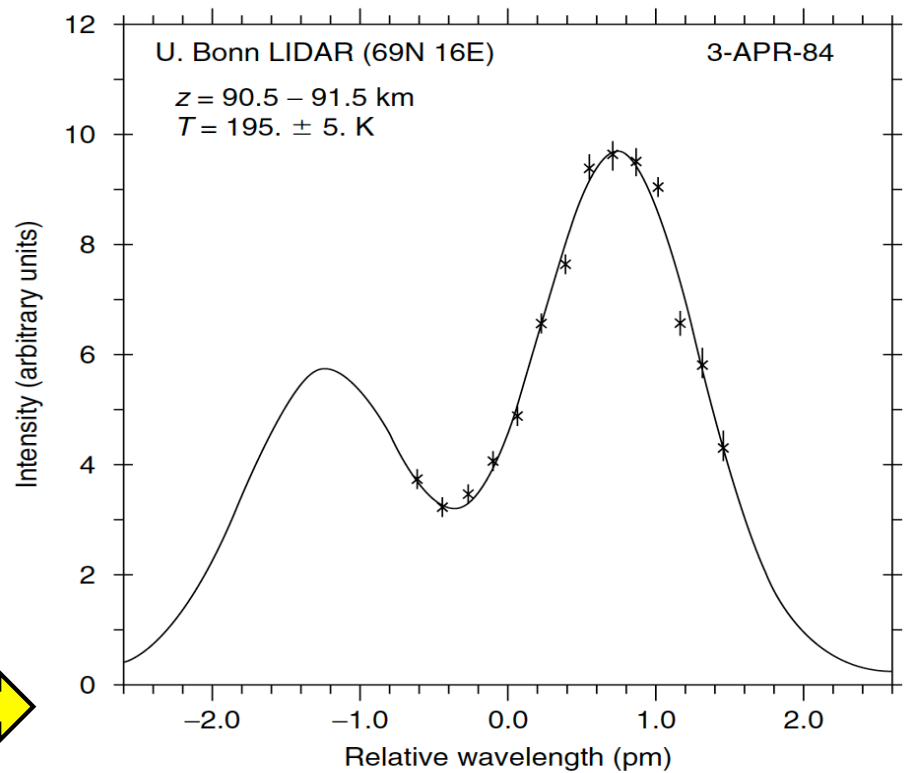
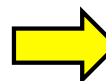
$$N_{Na}(\lambda, z) = \left(\frac{P_L(\lambda)\Delta t}{hc/\lambda} \right) (\sigma_{eff}(\lambda)n_{Na}(z)\Delta z) \left(\frac{A}{4\pi z^2} \right) \left(\eta(\lambda)T_a^2(\lambda)T_c^2(\lambda, z)G(z) \right) \quad (13.5)$$

$$N_R(\lambda, z_R) = \left(\frac{P_L(\lambda)\Delta t}{hc/\lambda} \right) (\sigma_R(\pi, \lambda)n_R(z_R)\Delta z) \left(\frac{A}{z_R^2} \right) \left(\eta(\lambda)T_a^2(\lambda, z_R)G(z_R) \right) \quad (13.6)$$

$$\sigma_{eff}(\lambda, z) = \frac{C(z)}{T_c^2(\lambda, z)} \frac{N_{Na}(\lambda, z)}{N_R(\lambda, z_R)} \quad (13.7)$$

$$\text{where } C(z) = \frac{\sigma_R(\pi, \lambda)n_R(z_R)}{n_{Na}(z)} \frac{4\pi z^2}{z_R^2} \quad (13.8)$$

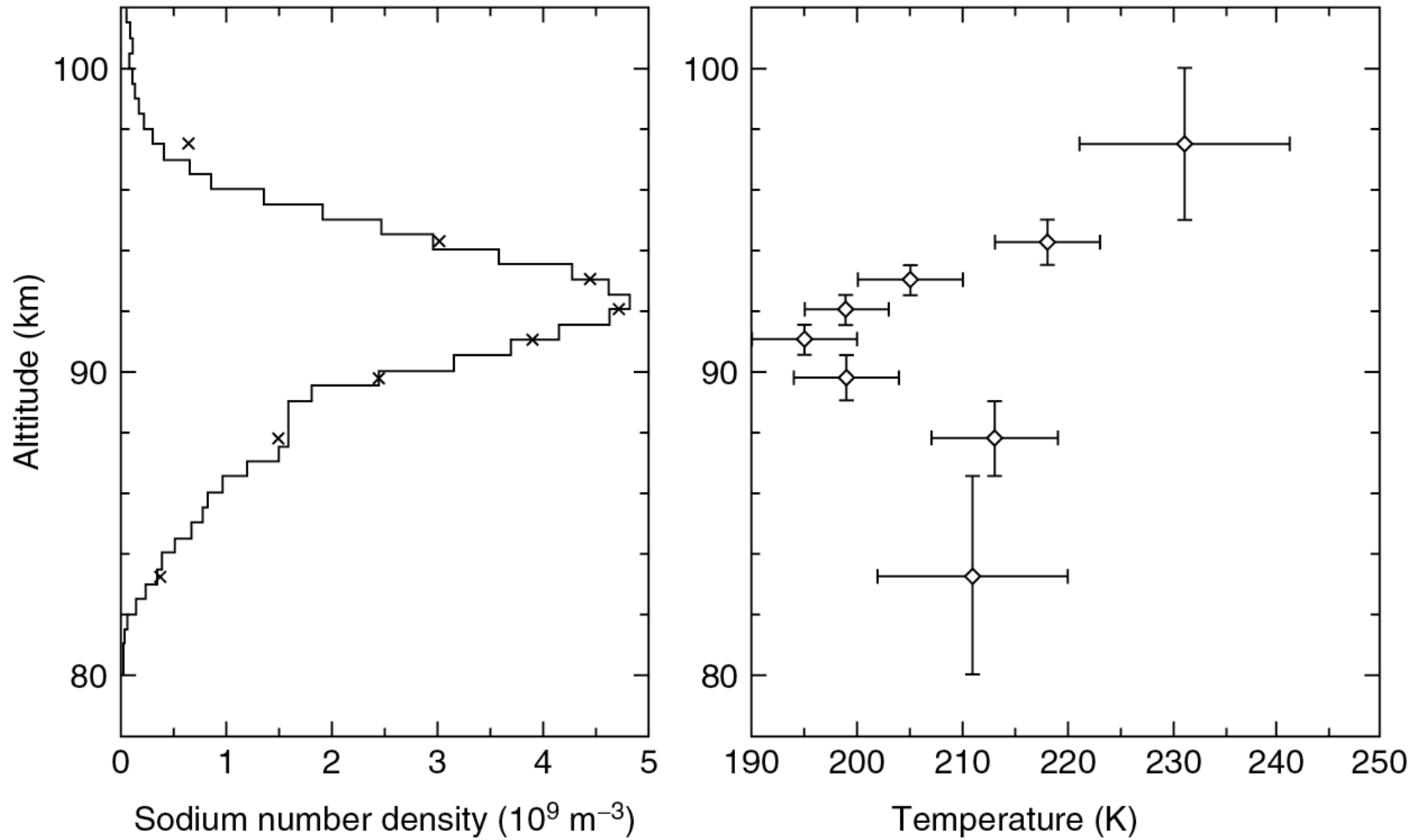
Least-square fitting gives temp
[Fricke and von Zahn, JATP, 1985]





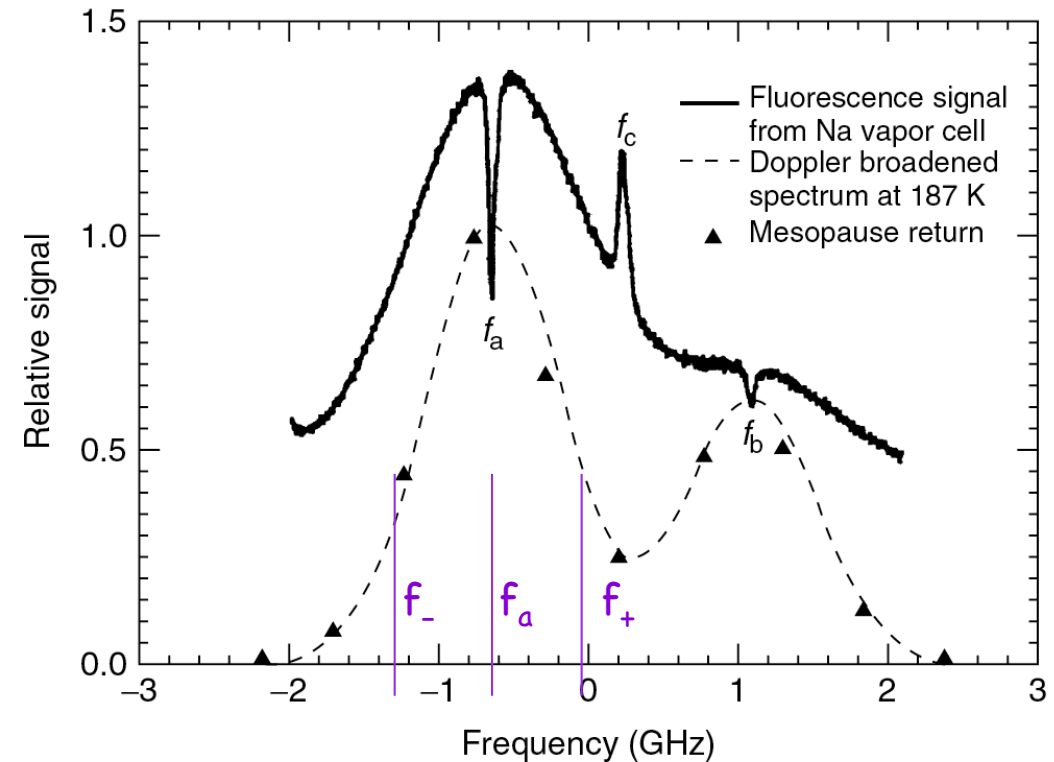
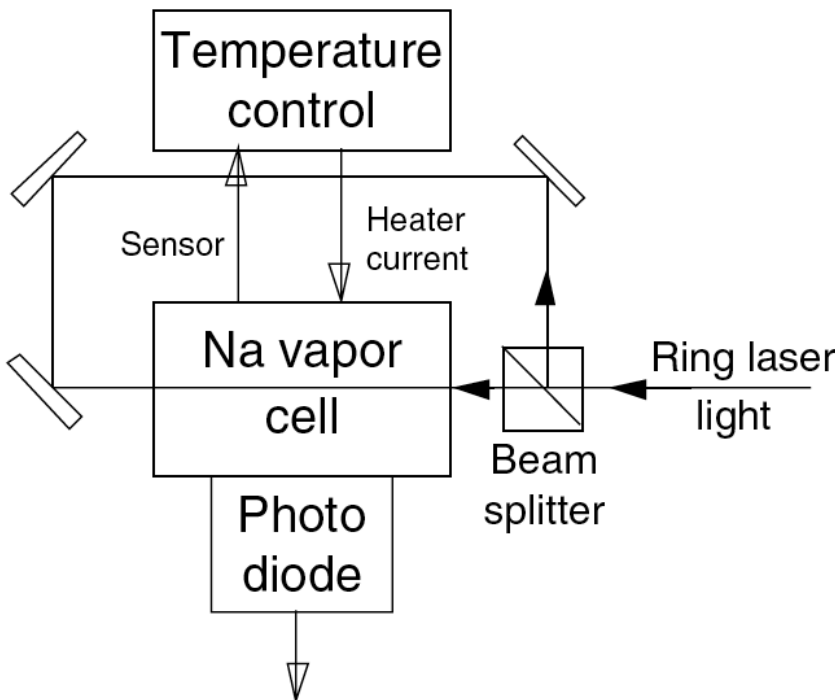
Scanning Na Lidar Results

U. Bonn LIDAR (69°N 16°E) 3. April 1984

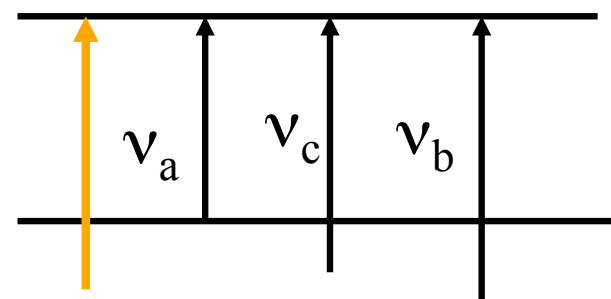




Doppler-Free Na Spectroscopy



See detailed explanation
on Na Doppler-free
saturation-fluorescence
spectroscopy in Textbook
Chapter 5.2.2.3.2

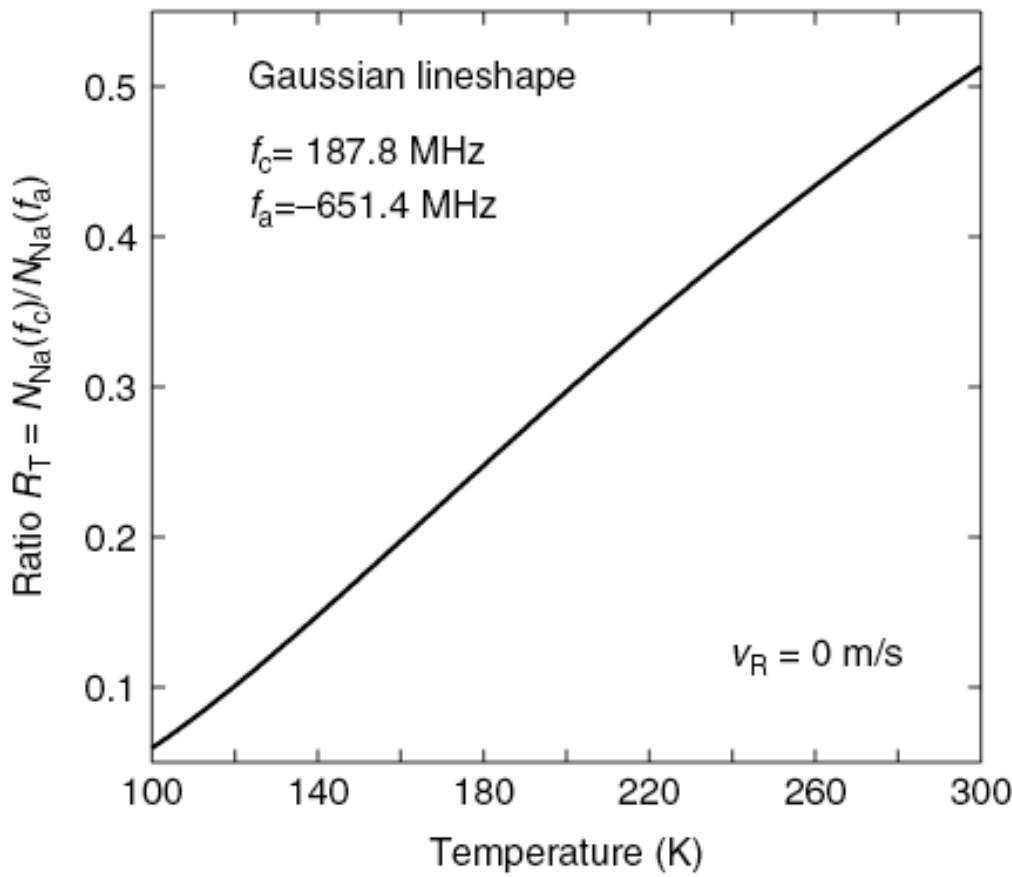


$$v_c = (v_a + v_b)/2 \quad (13.9)$$



2-Frequency Doppler Ratio Technique

$$R_T(z) = \frac{N_{norm}(f_c, z, t_1)}{N_{norm}(f_a, z, t_2)} = \frac{\sigma_{eff}(f_c, z) n_{Na}(z, t_1)}{\sigma_{eff}(f_a, z) n_{Na}(z, t_2)} \approx \frac{\sigma_{eff}(f_c, z)}{\sigma_{eff}(f_a, z)} \quad (13.10)$$



$$N_{norm}(f, z, t) \equiv \frac{N_{Na}(f, z, t)}{N_R(f, z, t) T_c^2(f, z)} \frac{z^2}{z_R^2} \quad (13.11)$$

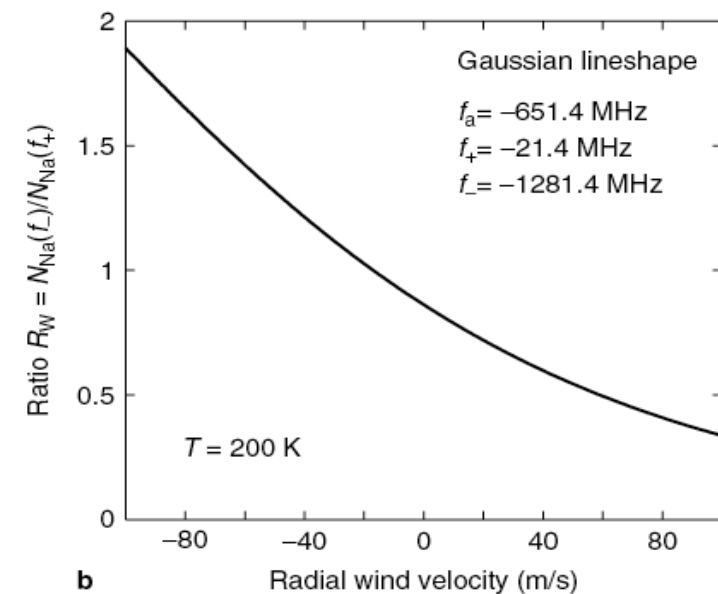
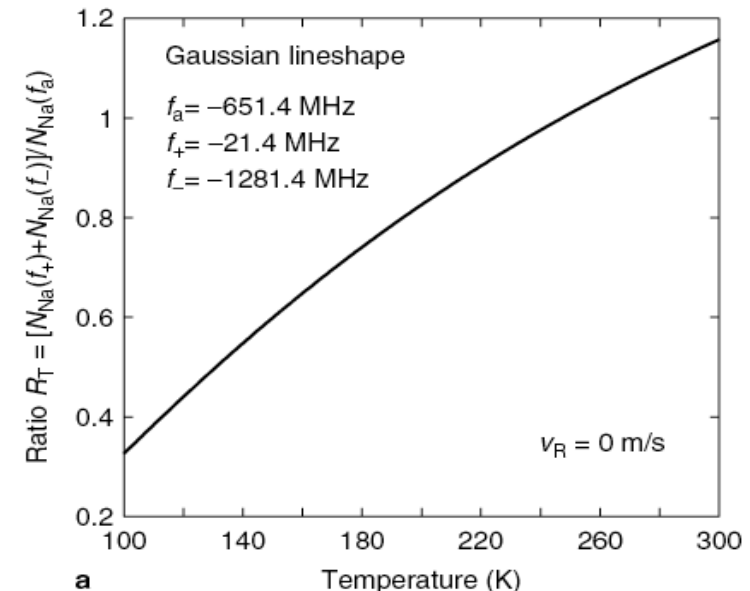
$$N_{norm}(f, z, t) = \frac{\sigma_{eff}(f) n_{Na}(z)}{\sigma_R(\pi, f) n_R(z_R)} \frac{1}{4\pi} \quad (13.12)$$



3-Frequency Doppler Ratio Technique

$$R_T(z) = \frac{N_{norm}(f_+, z, t_1) + N_{norm}(f_-, z, t_2)}{N_{norm}(f_a, z, t_3)}$$
$$\approx \frac{\sigma_{eff}(f_+, z) + \sigma_{eff}(f_-, z)}{\sigma_{eff}(f_a, z)} \quad (13.13)$$

$$R_W(z) = \frac{N_{norm}(f_-, z, t_2)}{N_{norm}(f_+, z, t_1)} \approx \frac{\sigma_{eff}(f_-, z)}{\sigma_{eff}(f_+, z)} \quad (13.14)$$





Main Ideas Behind Ratio Technique

- Three unknown parameters (temperature, radial wind, and Na number density) require 3 lidar equations at 3 frequencies as minimum \Rightarrow highest resolution.
- In the ratio technique, Na number density is cancelled out. So we have two ratios R_T and R_W that are independent of Na density but both dependent on T and W.
- The idea is to derive temperature and radial wind from these two ratios first, and then derive Na number density using computed temperature and wind at each altitude bin.
- However, because the Na extinction coefficient is involved, the upper bins are related to lower bins, and extinction coefficient is related to Na density and effective cross-section. The solution is to start from the bottom of the Na layer and then work bin by bin to the layer top.



Principle of Doppler Ratio Technique

- Lidar equation for resonance fluorescence (Na, K, or Fe)

$$N_S(\lambda, z) = \left(\frac{P_L(\lambda)\Delta t}{hc/\lambda} \right) \left[\sigma_{eff}(\lambda, z)n_c(z)R_B(\lambda) + \sigma_R(\pi, \lambda)n_R(z) \right] \Delta z \left(\frac{A}{4\pi z^2} \right) \\ \times \left(T_a^2(\lambda)T_c^2(\lambda, z) \right) (\eta(\lambda)G(z)) + N_B$$

$R_B = 1$ for current Na Doppler lidar since return photons at all wavelengths are received by the broadband receiver, so no fluorescence is filtered off.

- Pure Na signal and pure Rayleigh signal in Na region are

$$N_{Na}(\lambda, z) = \left(\frac{P_L(\lambda)\Delta t}{hc/\lambda} \right) \left[\sigma_{eff}(\lambda, z)n_c(z) \right] \Delta z \left(\frac{A}{4\pi z^2} \right) \left(T_a^2(\lambda)T_c^2(\lambda, z) \right) (\eta(\lambda)G(z))$$

$$N_R(\lambda, z) = \left(\frac{P_L(\lambda)\Delta t}{hc/\lambda} \right) \left[\sigma_R(\pi, \lambda)n_R(z) \right] \Delta z \left(\frac{A}{z^2} \right) \left(T_a^2(\lambda)T_c^2(\lambda, z) \right) (\eta(\lambda)G(z))$$

- So we have

$$N_S(\lambda, z) = N_{Na}(\lambda, z) + N_R(\lambda, z) + N_B$$



Principle of Doppler Ratio Technique

- Lidar equation at pure molecular scattering region (35–55km)

$$N_S(\lambda, z_R) = \left(\frac{P_L(\lambda)\Delta t}{hc/\lambda} \right) [\sigma_R(\pi, \lambda)n_R(z_R)] \Delta z \left(\frac{A}{z_R^2} \right) T_a^2(\lambda, z_R) (\eta(\lambda)G(z_R)) + N_B$$

- Pure Rayleigh signal in molecular scattering region is

$$N_R(\lambda, z_R) = \left(\frac{P_L(\lambda)\Delta t}{hc/\lambda} \right) [\sigma_R(\pi, \lambda)n_R(z_R)] \Delta z \left(\frac{A}{z_R^2} \right) T_a^2(\lambda, z_R) (\eta(\lambda)G(z_R))$$

- So we have

$$N_S(\lambda, z_R) = N_R(\lambda, z_R) + N_B$$

- The ratio between Rayleigh signals at z and z_R is given by

$$\frac{N_R(\lambda, z)}{N_R(\lambda, z_R)} = \frac{[\sigma_R(\pi, \lambda)n_R(z)]T_a^2(\lambda, z)T_c^2(\lambda, z)G(z)}{[\sigma_R(\pi, \lambda)n_R(z_R)]T_a^2(\lambda, z_R)G(z_R)} \frac{z_R^2}{z^2} = \frac{n_R(z)}{n_R(z_R)} \frac{z_R^2}{z^2} T_c^2(\lambda, z)$$

Where n_R is the (total) atmospheric number density, usually obtained from atmospheric models like MSIS00.



Principle of Doppler Ratio Technique

- From above equations, the pure Na and Rayleigh signals are

$$N_{Na}(\lambda, z) = N_S(\lambda, z) - N_B - N_R(\lambda, z)$$

$$N_R(\lambda, z_R) = N_S(\lambda, z_R) - N_B$$

- Normalized Na photon count is defined as

$$N_{Norm}(\lambda, z) = \frac{N_{Na}(\lambda, z)}{N_R(\lambda, z_R) T_c^2(\lambda, z)} \frac{z^2}{z_R^2}$$

- From physics point of view, the normalized Na count is

$$N_{Norm}(\lambda, z) = \frac{N_{Na}(\lambda, z)}{N_R(\lambda, z_R) T_c^2(\lambda, z)} = \frac{\sigma_{eff}(\lambda, z) n_c(z)}{\sigma_R(\pi, \lambda) n_R(z_R)} \frac{1}{4\pi}$$

- From actual photon counts, the normalized Na count is

$$\begin{aligned} N_{Norm}(\lambda, z) &= \frac{N_{Na}(\lambda, z)}{N_R(\lambda, z_R) T_c^2(\lambda, z)} \frac{z^2}{z_R^2} = \frac{N_S(\lambda, z) - N_B - N_R(\lambda, z)}{N_R(\lambda, z_R) T_c^2(\lambda, z)} \frac{z^2}{z_R^2} \\ &= \frac{N_S(\lambda, z) - N_B}{N_S(\lambda, z_R) - N_B} \frac{z^2}{z_R^2} \frac{1}{T_c^2(\lambda, z)} - \frac{n_R(z)}{n_R(z_R)} \end{aligned}$$



Principle of Doppler Ratio Technique

- From physics, the ratios of R_T and R_W are then given by

$$R_T = \frac{N_{Norm}(f_+, z) + N_{Norm}(f_-, z)}{N_{Norm}(f_a, z)} = \frac{\frac{\sigma_{eff}(f_+, z)n_c(z)}{\sigma_R(\pi, f_+)n_R(z_R)} + \frac{\sigma_{eff}(f_-, z)n_c(z)}{\sigma_R(\pi, f_-)n_R(z_R)}}{\frac{\sigma_{eff}(f_a, z)n_c(z)}{\sigma_R(\pi, f_a)n_R(z_R)}} = \frac{\sigma_{eff}(f_+, z) + \sigma_{eff}(f_-, z)}{\sigma_{eff}(f_a, z)}$$

$$R_W = \frac{N_{Norm}(f_+, z) - N_{Norm}(f_-, z)}{N_{Norm}(f_a, z)} = \frac{\frac{\sigma_{eff}(f_+, z)n_c(z)}{\sigma_R(\pi, f_+)n_R(z_R)} - \frac{\sigma_{eff}(f_-, z)n_c(z)}{\sigma_R(\pi, f_-)n_R(z_R)}}{\frac{\sigma_{eff}(f_a, z)n_c(z)}{\sigma_R(\pi, f_a)n_R(z_R)}} = \frac{\sigma_{eff}(f_+, z) - \sigma_{eff}(f_-, z)}{\sigma_{eff}(f_a, z)}$$

Here, Rayleigh backscatter cross-section is regarded as the same for three frequencies, since the frequency difference is so small. Na number density is also the same for three frequency channels, and so is the atmosphere number density at Rayleigh normalization altitude.



Principle of Doppler Ratio Technique

- From actual photon counts, the ratios R_T and R_W are

$$R_T = \frac{N_{Norm}(f_+, z) + N_{Norm}(f_-, z)}{N_{Norm}(f_a, z)}$$
$$= \frac{\left(\frac{N_S(f_+, z) - N_B}{N_S(f_+, z_R) - N_B} \frac{z^2}{z_R^2} \frac{1}{T_c^2(f_+, z)} - \frac{n_R(z)}{n_R(z_R)} \right) + \left(\frac{N_S(f_-, z) - N_B}{N_S(f_-, z_R) - N_B} \frac{z^2}{z_R^2} \frac{1}{T_c^2(f_-, z)} - \frac{n_R(z)}{n_R(z_R)} \right)}{\frac{N_S(f_a, z) - N_B}{N_S(f_a, z_R) - N_B} \frac{z^2}{z_R^2} \frac{1}{T_c^2(f_a, z)} - \frac{n_R(z)}{n_R(z_R)}}$$

$$R_W = \frac{N_{Norm}(f_+, z) - N_{Norm}(f_-, z)}{N_{Norm}(f_a, z)}$$
$$= \frac{\left(\frac{N_S(f_+, z) - N_B}{N_S(f_+, z_R) - N_B} \frac{z^2}{z_R^2} \frac{1}{T_c^2(f_+, z)} - \frac{n_R(z)}{n_R(z_R)} \right) - \left(\frac{N_S(f_-, z) - N_B}{N_S(f_-, z_R) - N_B} \frac{z^2}{z_R^2} \frac{1}{T_c^2(f_-, z)} - \frac{n_R(z)}{n_R(z_R)} \right)}{\frac{N_S(f_a, z) - N_B}{N_S(f_a, z_R) - N_B} \frac{z^2}{z_R^2} \frac{1}{T_c^2(f_a, z)} - \frac{n_R(z)}{n_R(z_R)}}$$



How Does Ratio Technique Work?

- From physics, we calculate the ratios of R_T and R_W as

$$R_T = \frac{\sigma_{eff}(f_+, z) + \sigma_{eff}(f_-, z)}{\sigma_{eff}(f_a, z)}$$

$$R_W = \frac{\sigma_{eff}(f_+, z) - \sigma_{eff}(f_-, z)}{\sigma_{eff}(f_a, z)}$$

- From actual photon counts, we calculate the ratios as

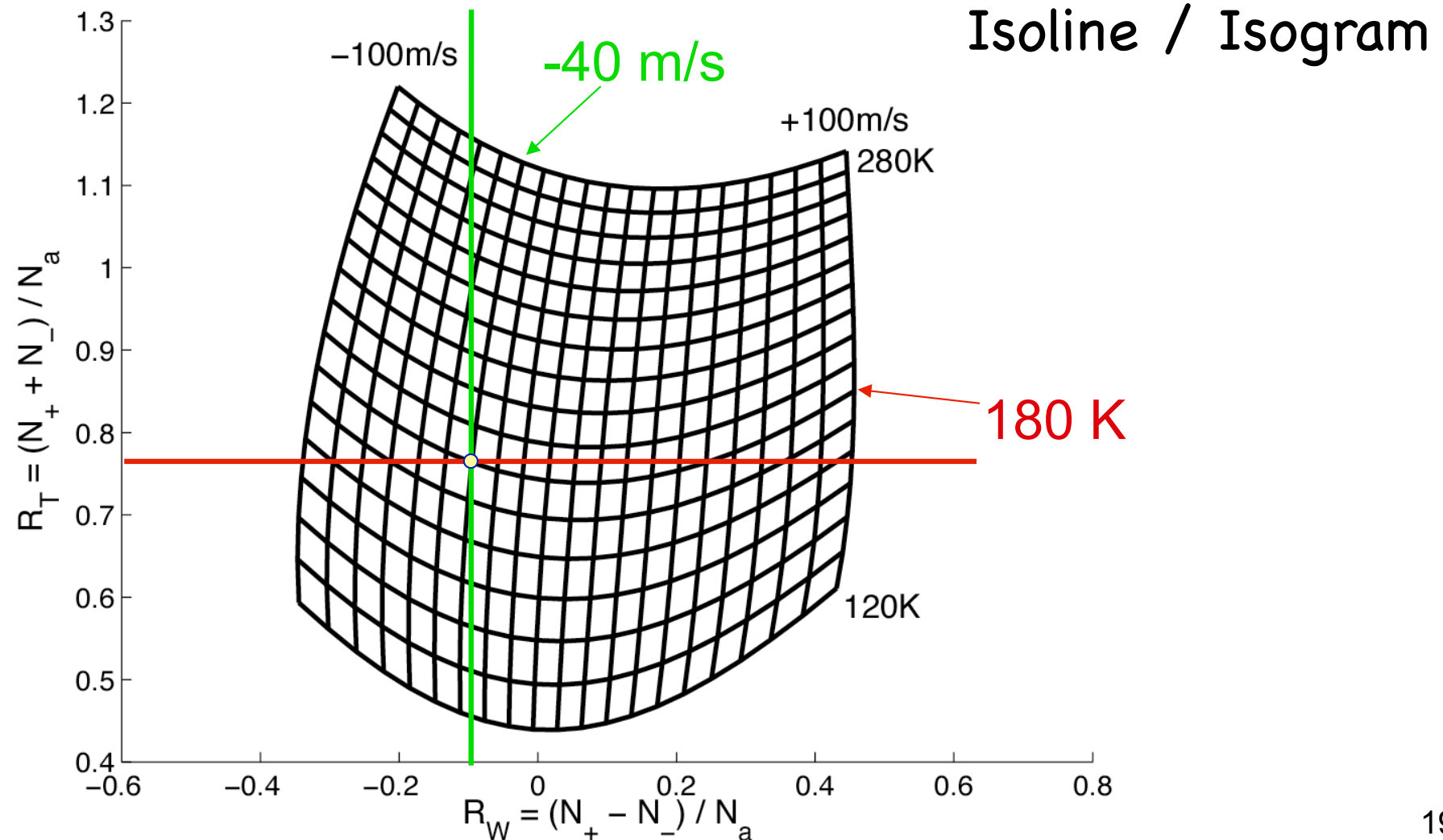
$$\begin{aligned} R_T &= \frac{N_{Norm}(f_+, z) + N_{Norm}(f_-, z)}{N_{Norm}(f_a, z)} \\ &= \frac{\left(\frac{N_S(f_+, z) - N_B}{N_S(f_+, z_R) - N_B} \frac{z^2}{z_R^2} \frac{1}{T_c^2(f_+, z)} - \frac{n_R(z)}{n_R(z_R)} \right) + \left(\frac{N_S(f_-, z) - N_B}{N_S(f_-, z_R) - N_B} \frac{z^2}{z_R^2} \frac{1}{T_c^2(f_-, z)} - \frac{n_R(z)}{n_R(z_R)} \right)}{\frac{N_S(f_a, z) - N_B}{N_S(f_a, z_R) - N_B} \frac{z^2}{z_R^2} \frac{1}{T_c^2(f_a, z)} - \frac{n_R(z)}{n_R(z_R)}} \end{aligned}$$

$$\begin{aligned} R_W &= \frac{N_{Norm}(f_+, z) - N_{Norm}(f_-, z)}{N_{Norm}(f_a, z)} \\ &= \frac{\left(\frac{N_S(f_+, z) - N_B}{N_S(f_+, z_R) - N_B} \frac{z^2}{z_R^2} \frac{1}{T_c^2(f_+, z)} - \frac{n_R(z)}{n_R(z_R)} \right) - \left(\frac{N_S(f_-, z) - N_B}{N_S(f_-, z_R) - N_B} \frac{z^2}{z_R^2} \frac{1}{T_c^2(f_-, z)} - \frac{n_R(z)}{n_R(z_R)} \right)}{\frac{N_S(f_a, z) - N_B}{N_S(f_a, z_R) - N_B} \frac{z^2}{z_R^2} \frac{1}{T_c^2(f_a, z)} - \frac{n_R(z)}{n_R(z_R)}} \end{aligned}$$



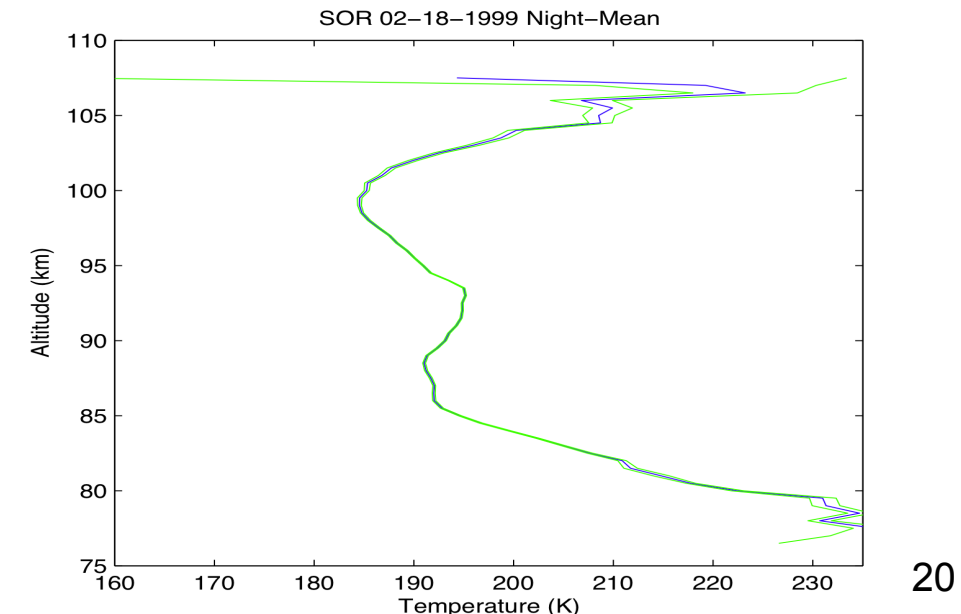
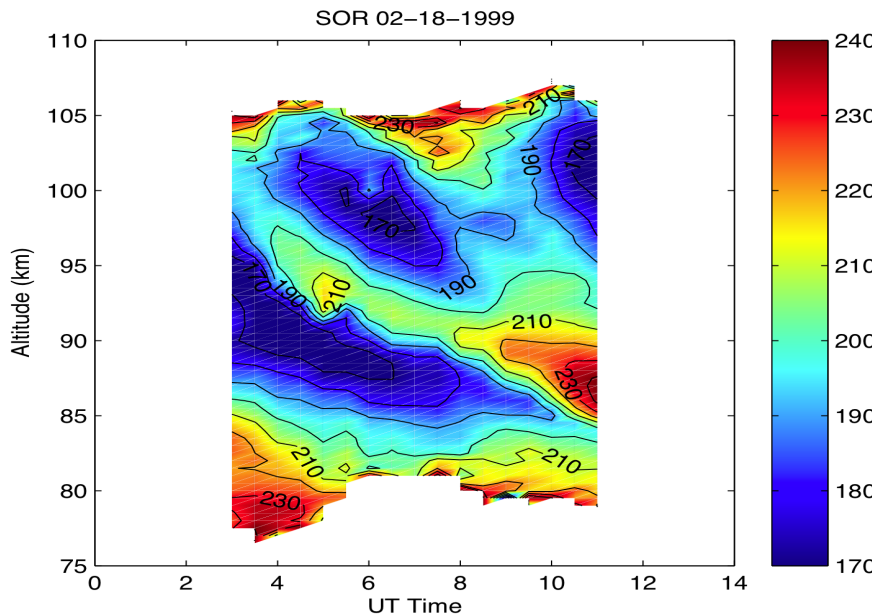
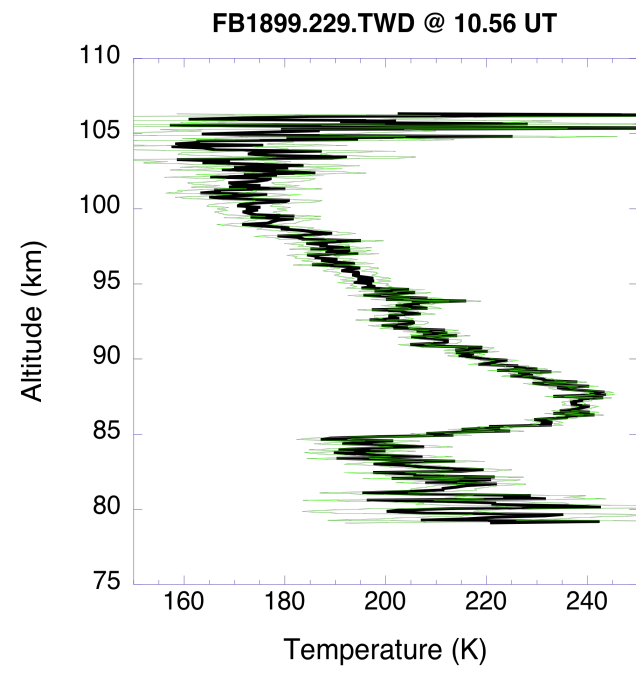
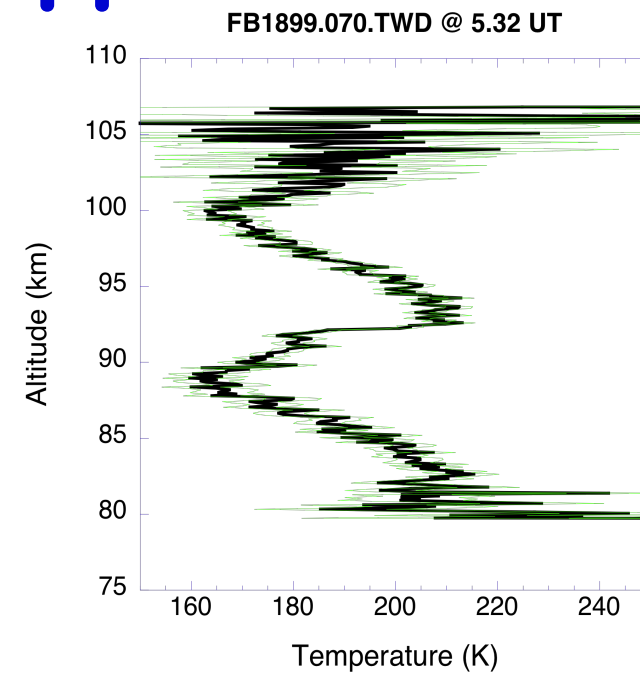
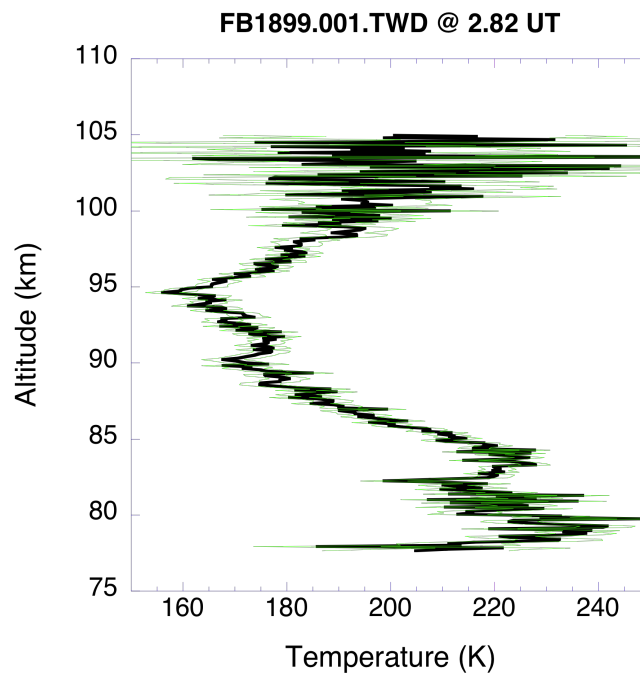
How Does Ratio Technique Work?

- Compute Doppler calibration curves from physics
- Look up these two ratios on the calibration curves to infer the corresponding Temperature and Wind from isoline/isogram.





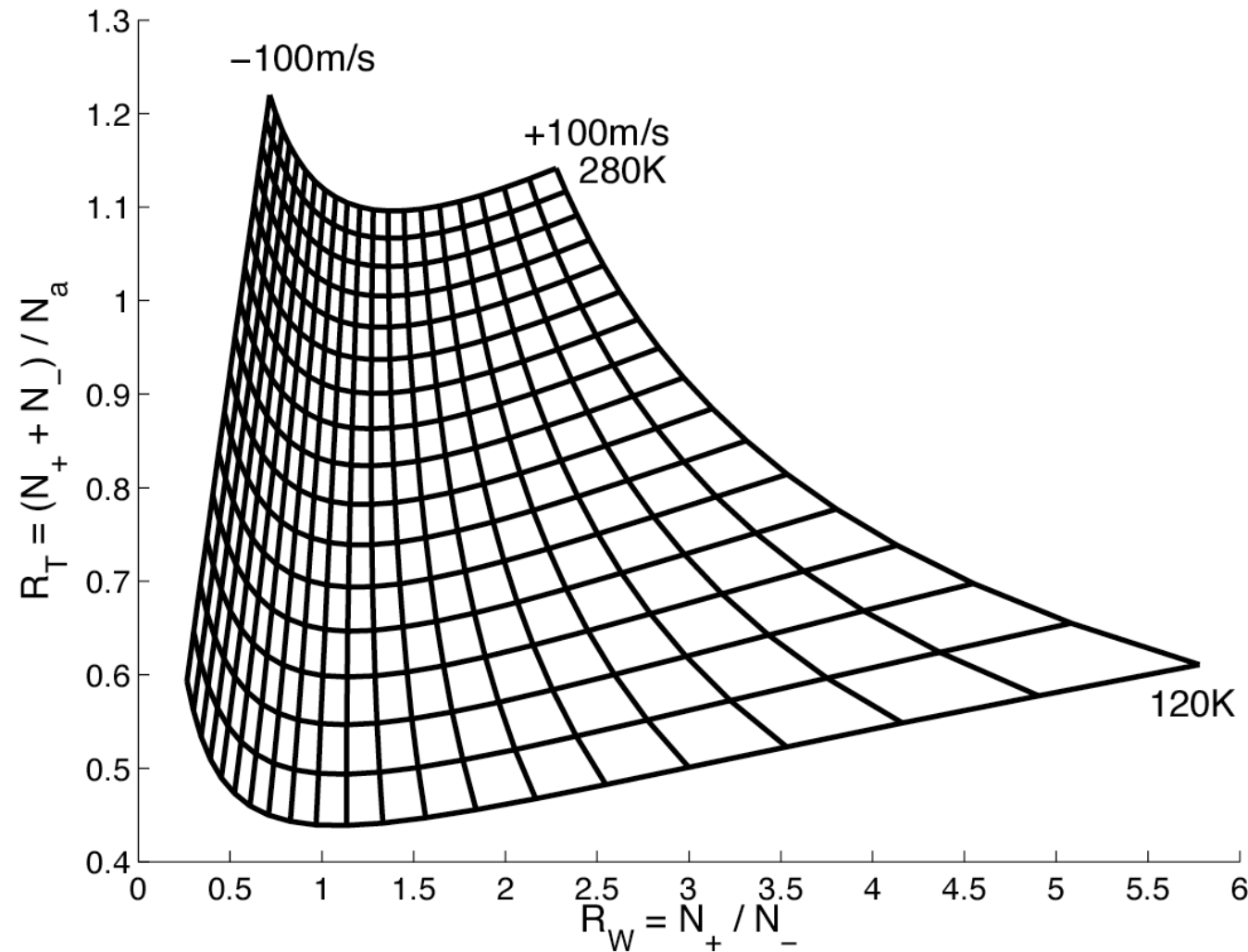
UIUC Na Doppler Lidar Data @ SOR





Comparison of Calibration Curves

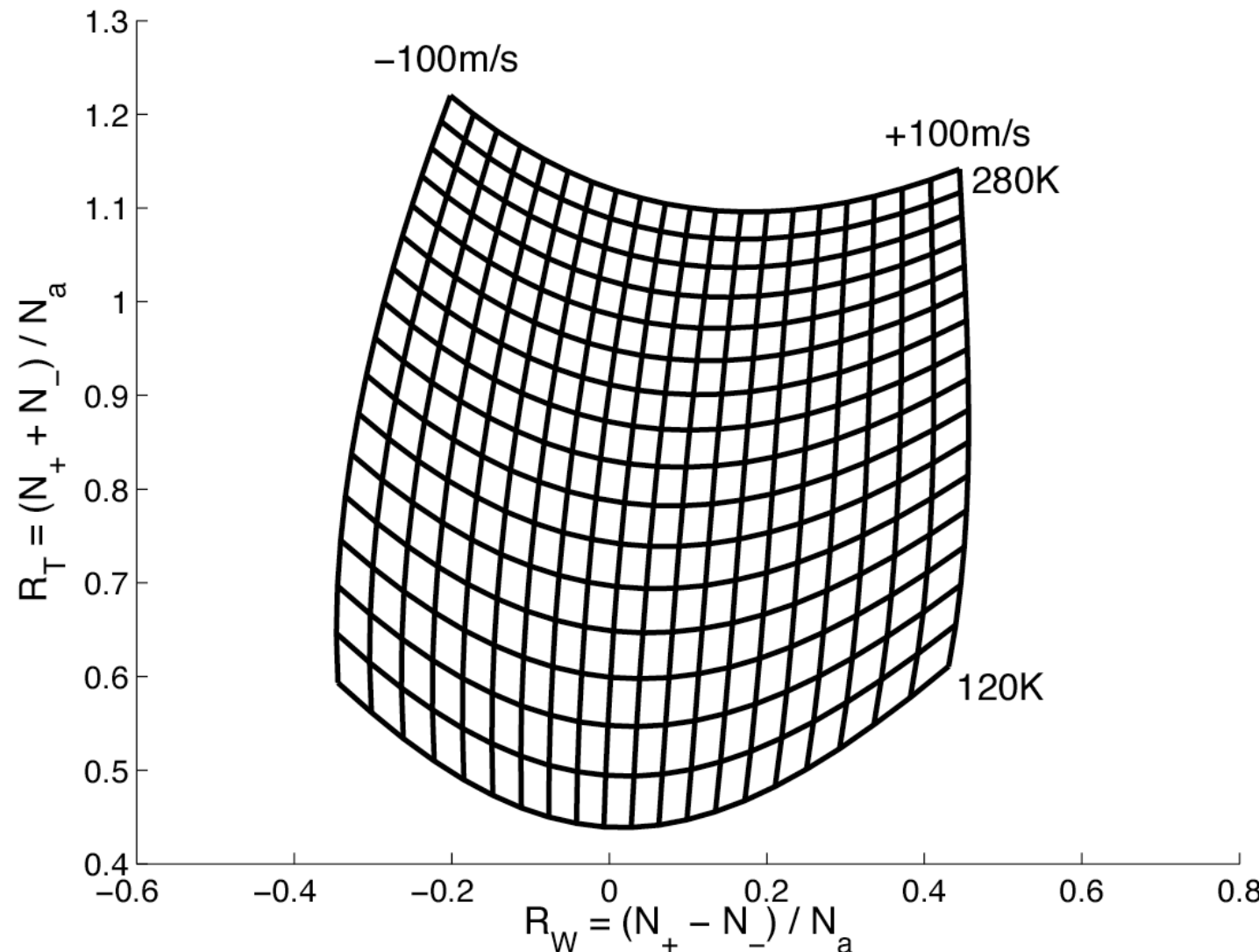
- Different metrics of R_w result in different wind sensitivities
- The ratio $R_w = N_+ / N_-$ has inhomogeneous sensitivity





Comparison of Calibration Curves

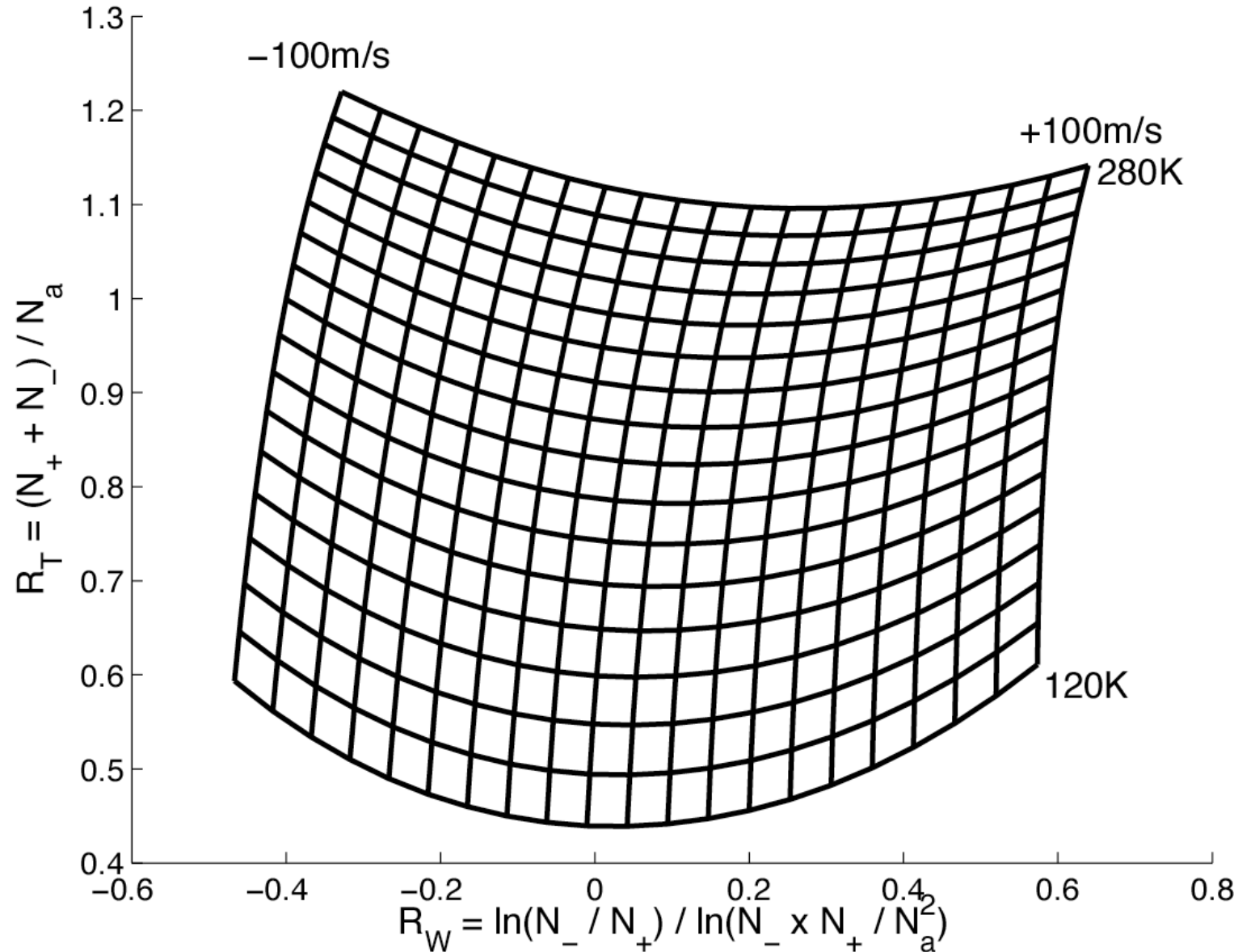
- The ratio $R_W = (N_+ - N_-)/N_a$ has much better uniformity than the simplest ratio





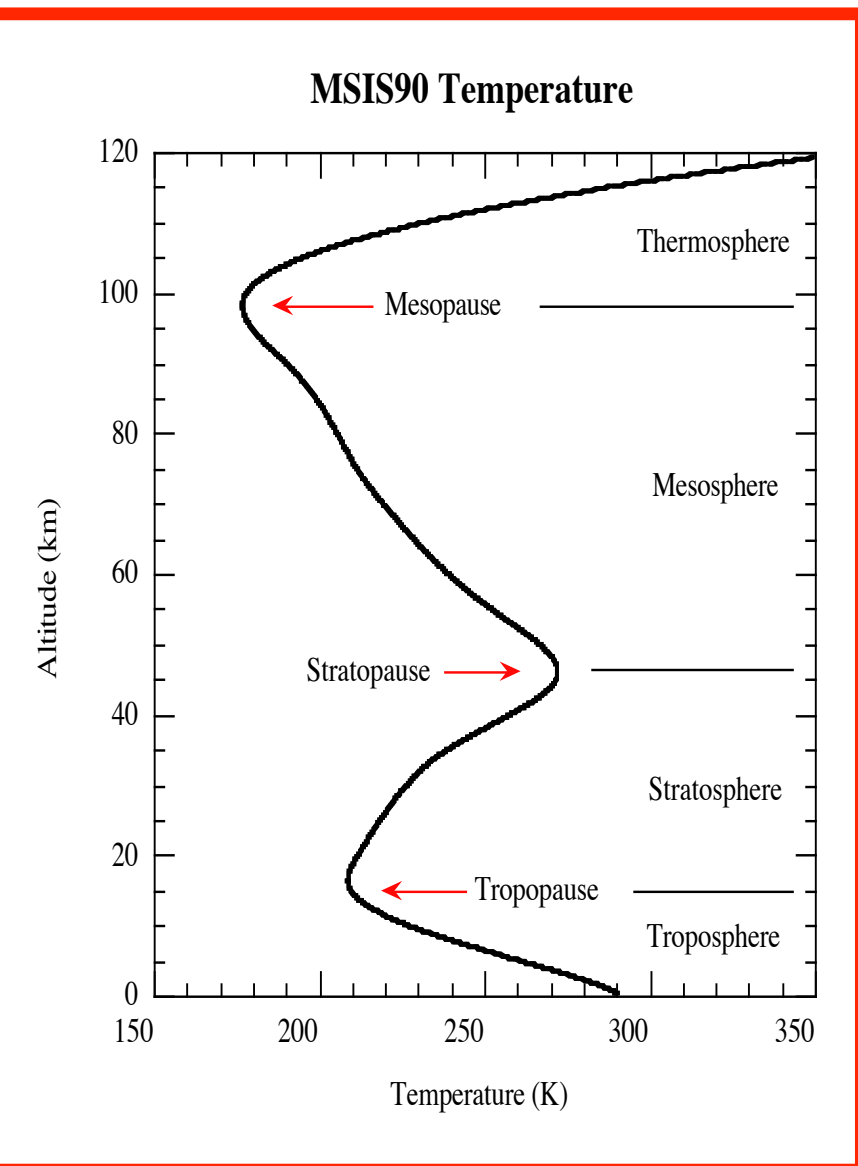
Comparison of Calibration Curves

- The ratio $R_w = \ln(N_- / N_+) / \ln(N_- \times N_+ / N_a^2)$ has good uniformity

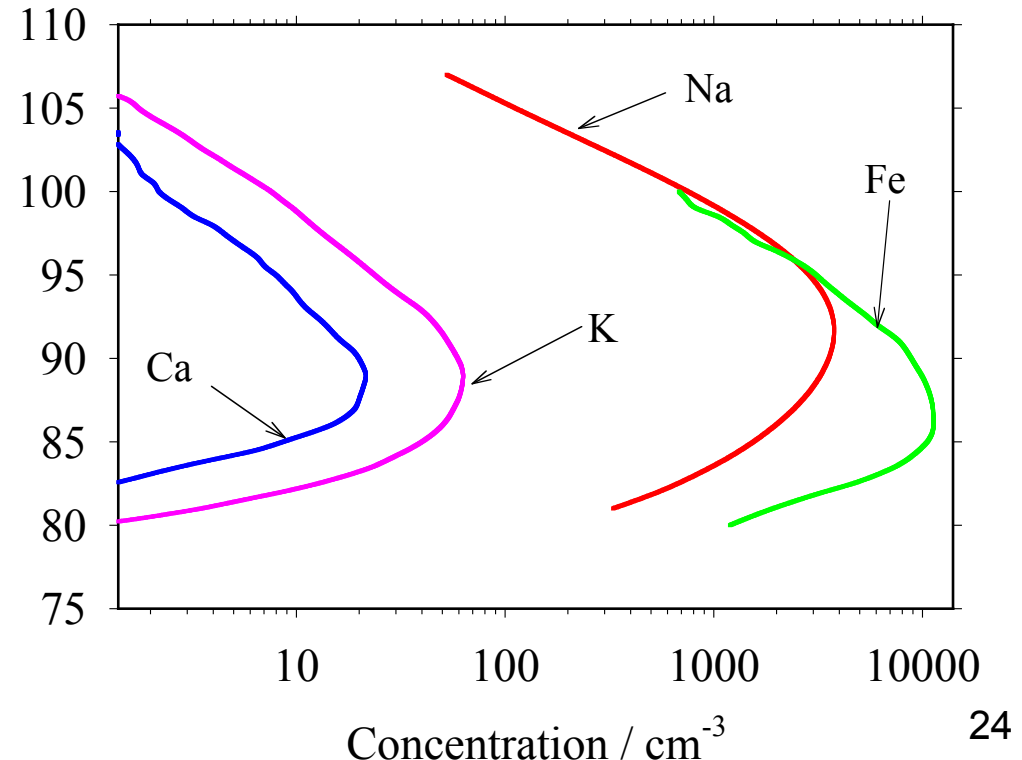




More Resonance Fluorescence Doppler Lidars



❑ Besides Na, there are more metal species (K, Fe, Ca, Ca⁺, Mg, Li, ...) from meteor ablation. They can be used as tracers for Doppler lidar measurements in MLT region.





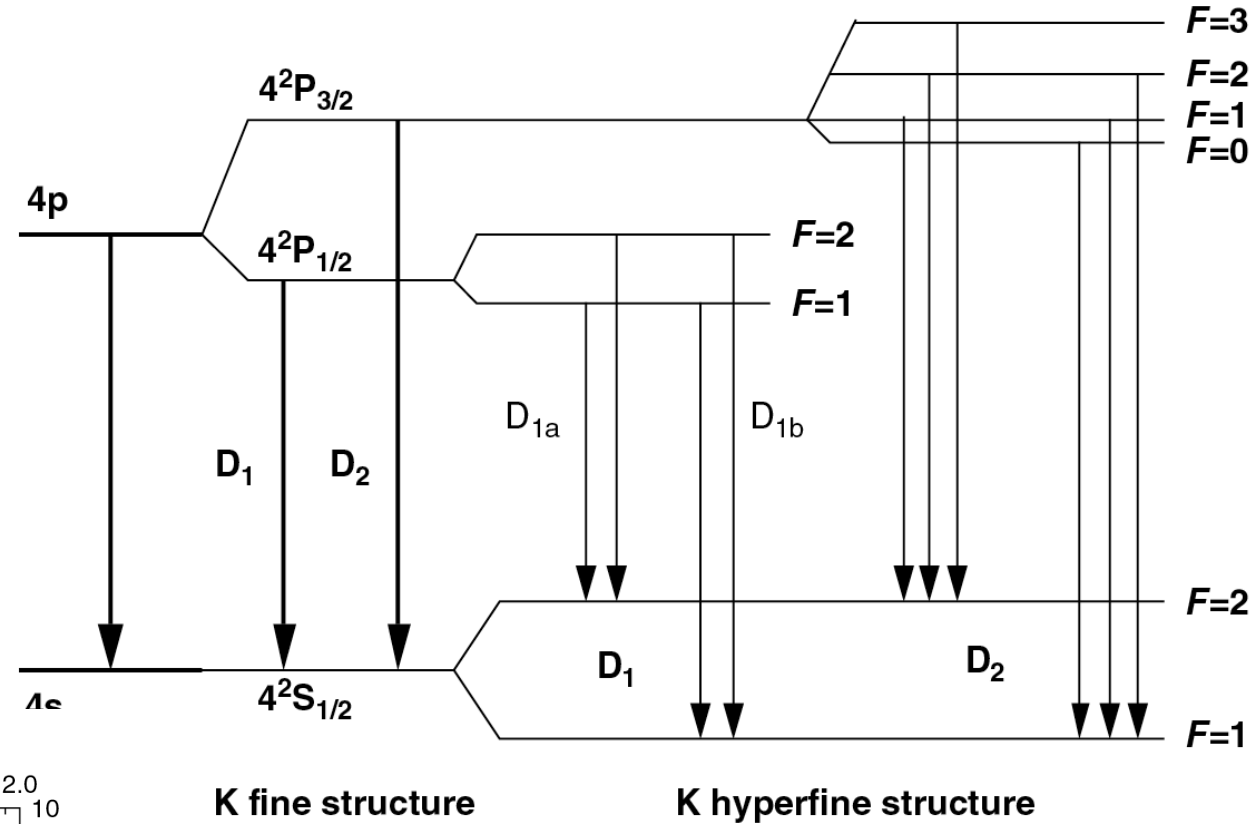
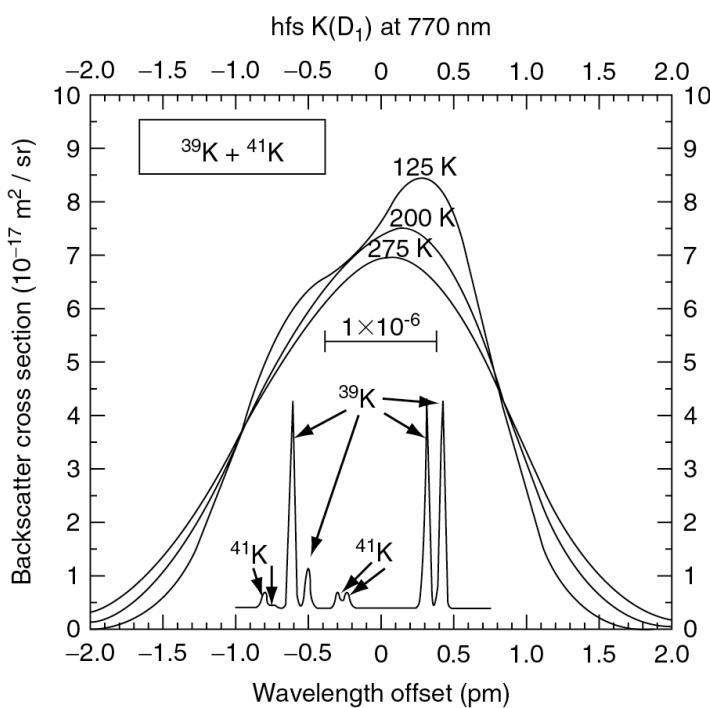
Metal Species in MLT Region

Species	Central wavelength (nm)	A_{ki} ($\times 10^8$ s $^{-1}$)	Degeneracy g _k / g _i	Atomic Weight	Isotopes	Doppler rms Width (MHz)	σ_0 ($\times 10^{-12}$ cm 2)	Abundance ($\times 10^9$ cm $^{-2}$)	Centroid Altitude (km)	Layer rms Width (km)
Na (D ₂)	589.1583	0.616	4 / 2	22.98977	23	456.54	14.87	4.0	91.5	4.6
Fe	372.0995	0.163	11 / 9	55.845	54, 56, 57, 58	463.79	0.944	10.2	88.3	4.5
K (D ₁)	770.1088	0.382	2 / 2	39.0983	39, 40, 41	267.90	13.42	4.5 x 10 $^{-2}$	91.0	4.7
K (D ₂)	766.702	0.387	4 / 2	39.0983	39, 40, 41	267.90	26.92	4.5 x 10 $^{-2}$	91.0	4.7
Ca	422.793	2.18	3 / 1	40.078	40, 42, 43, 44, 46, 48	481.96	38.48	3.4 x 10 $^{-2}$	90.5	3.5
Ca ⁺	393.777	1.47	4 / 2	40.078	Same as Ca	517.87	13.94	7.2 x 10 $^{-2}$	95.0	3.6

- ❑ In principle, all these species can be used as trace atoms for resonance fluorescence Doppler lidar measurements.
- ❑ Whether a Doppler lidar can be developed and used mainly depends on the availability and readiness of laser and electro-optic technologies. In addition, the constituent abundance and absorption cross-section are naturally determined.



K Atomic Energy Levels



Transition	K(D_1)	K(D_2)
Wavelength air [nm]	769.8974	766.4911
Wavelength vacuum [nm]	770.1093	766.7021
Rel. intensity	24	25
$A_{ik} [10^8 \text{s}^{-1}]$	$0.382 (\pm 10\%)$	$0.387 (\pm 10\%)$
f -value	0.340	0.682
Terms ${}^2S_{1/2} - {}^2P_{1/2}^o$	${}^2S_{1/2} - {}^2P_{3/2}^o$	
$g_i - g_k$	2-2	2-4



K Atomic Parameters

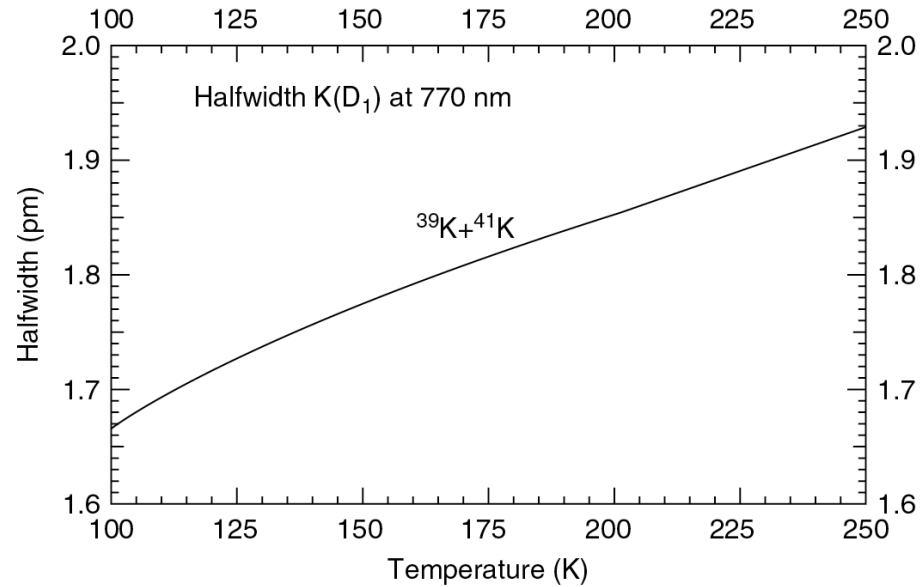
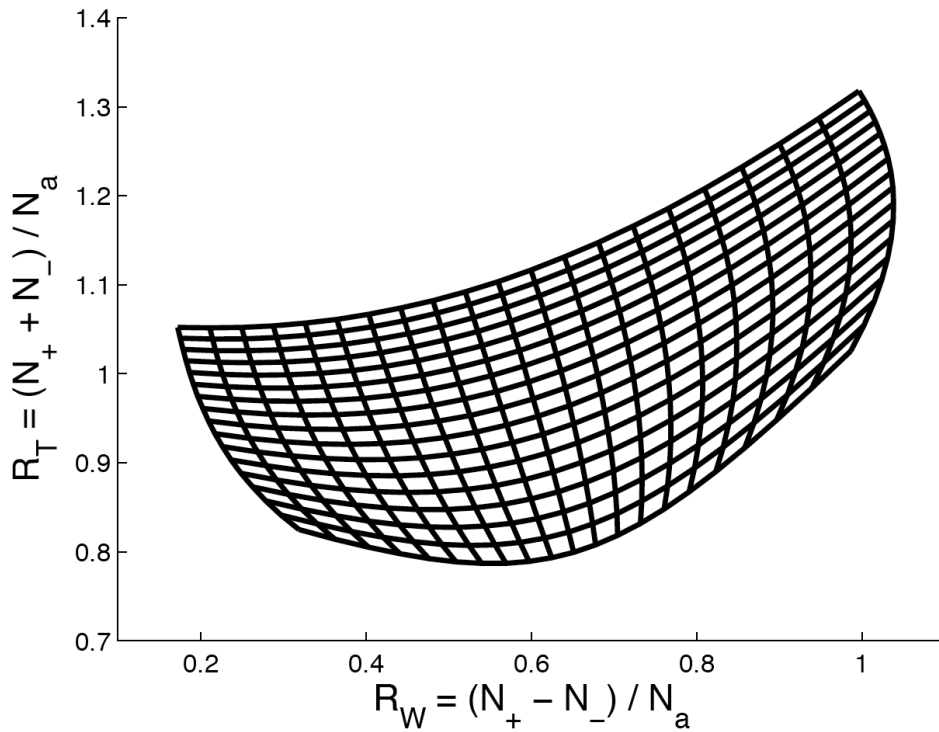
Isotope	Atomic mass	Abundance	Nuclear spin	K(D ₁) line shift
39	38.963 706 9(3)	0.932 581(44)	$I = 3/2$	0
40	39.963 998 67(29)	0.000 117(1)	$I = 4$	125.58 MHz
41	40.961 825 97(28)	0.067 302(44)	$I = 3/2$	235.28 MHz

Table 5.8 Quantum Numbers, Frequency Offsets, and Relative Line Strength for K (D₁) Hyperfine Structure Lines

² S _{1/2}	² P _{1/2}	³⁹ K (MHz)	⁴¹ K (MHz)	Relative Line Strength
$F = 1$	$F = 2$	310	405	5/16
	$F = 1$	254	375	1/16
$F = 2$	$F = 2$	-152	151	5/16
	$F = 1$	-208	121	5/16



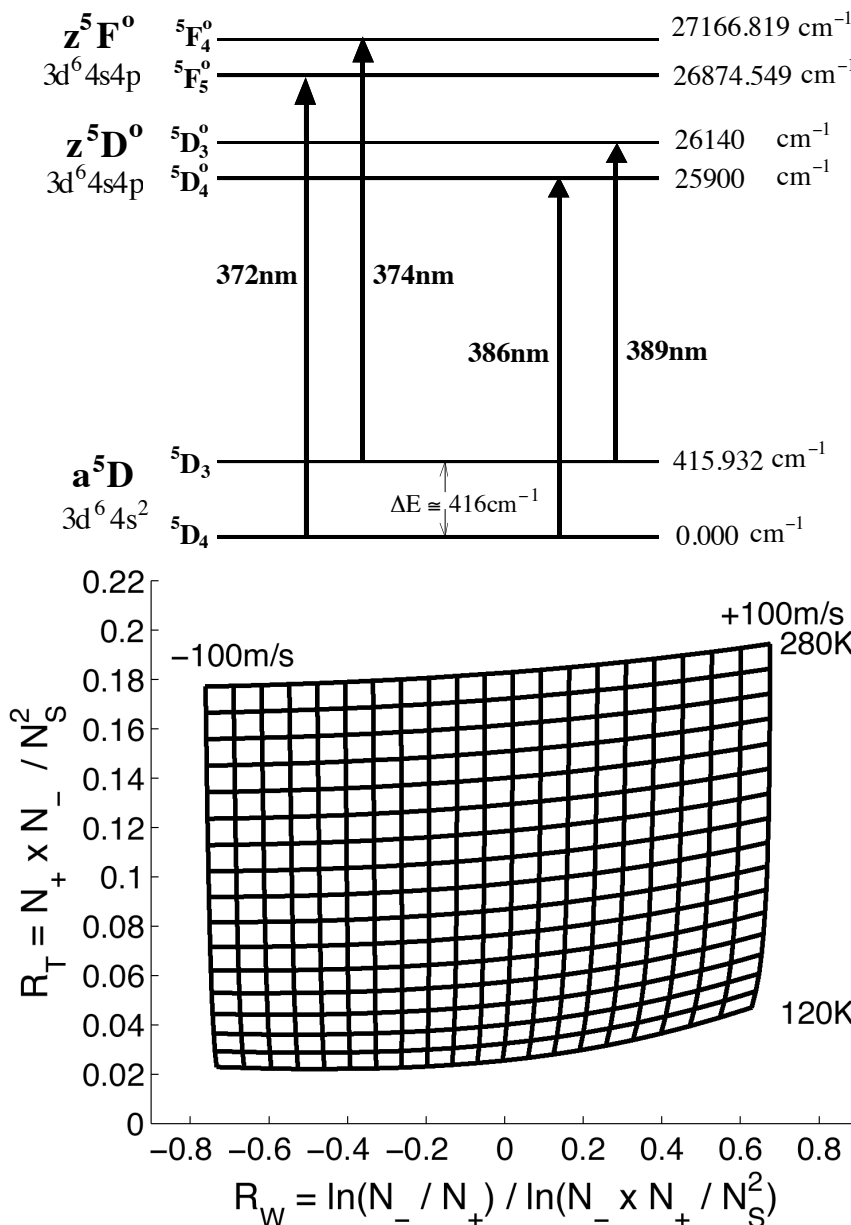
K Doppler Lidar Principle & Metrics



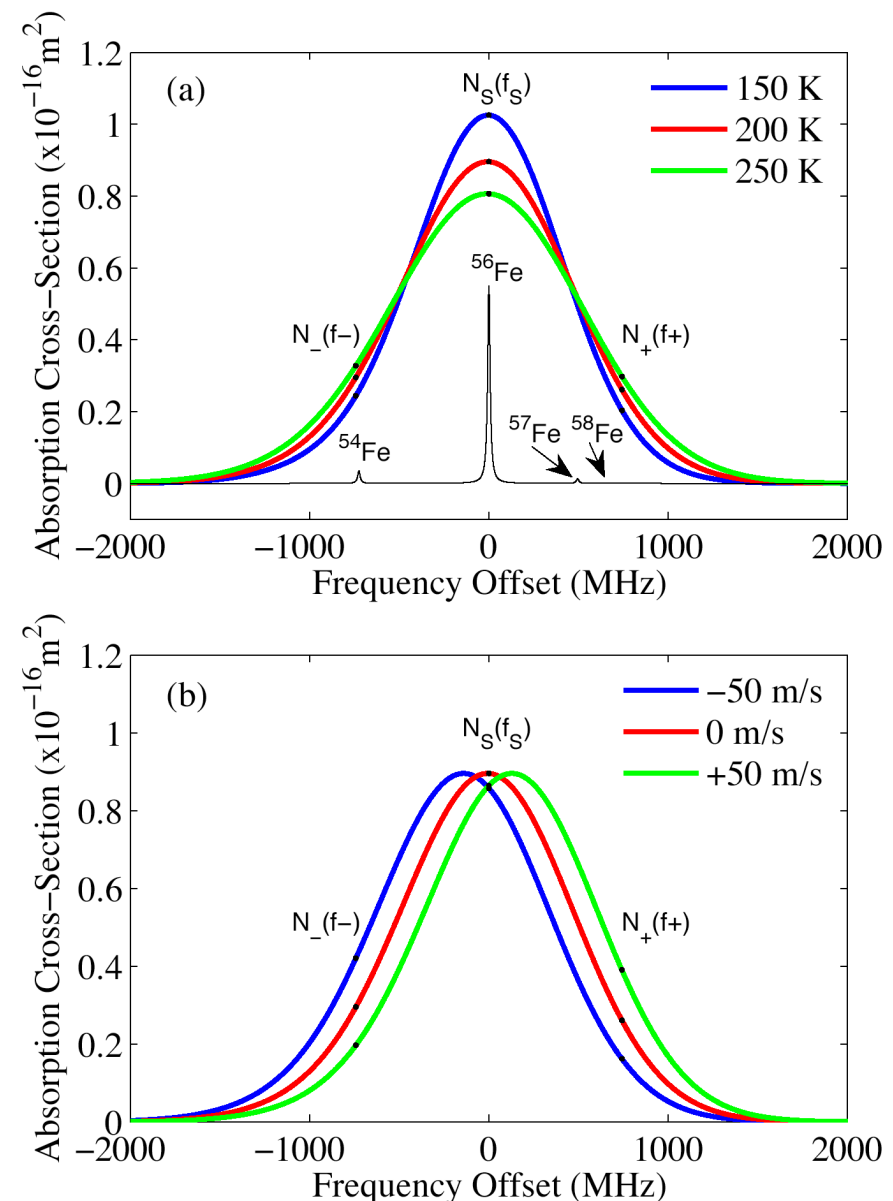
- ❑ Ratio technique versus scanning technique
- ❑ Scanning technique actually has its advantages on several aspects, depending on the laser system used - whether there is pedestal, background problems, etc.
- ❑ Ratio technique usually gives higher resolution.



Fe Doppler Lidar Principles



[Chu et al., ILRC, 2008]

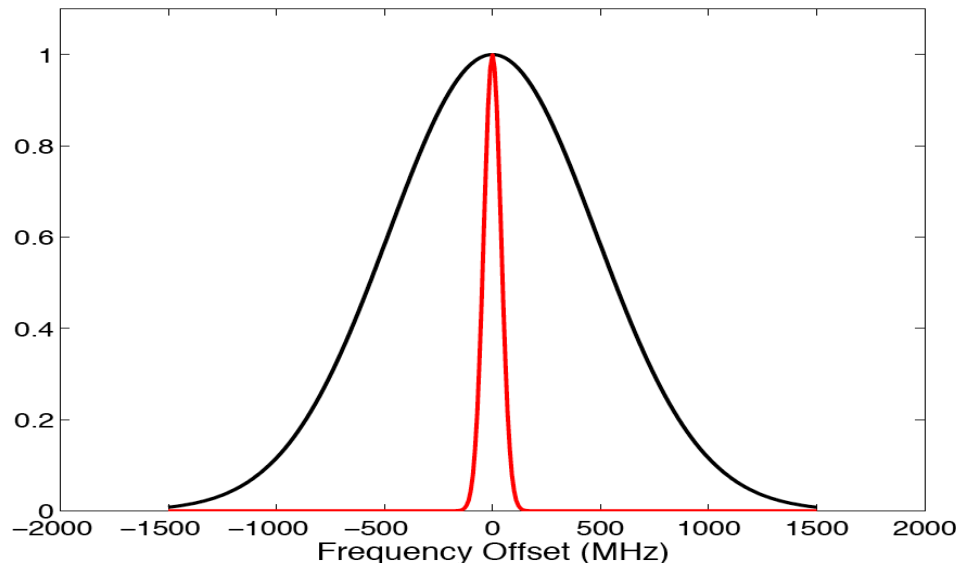


Fe (iron) 372-nm line



Effective Cross Section Computation

- The effective cross section is a convolution of the atomic absorption cross section and the laser line shape.



For Gaussian shapes of atomic absorption and laser lineshape:

$$\sigma_e = \sqrt{\sigma_D^2 + \sigma_L^2}$$

- How would you calculate the effective cross section when atoms have isotopes, e.g., K (potassium) or Fe (iron)?

$$\sigma_{eff}(\text{overall}) = \sum_{m=1}^N [\sigma_{eff,m}(\text{isotope}) \times \text{Isotope Abdn}_m]$$



Summary (1)

- ❑ Resonance fluorescence Doppler lidars apply Doppler technique to infer temperature and wind from the Doppler-broadened and Doppler-shifted atomic absorption spectroscopy. The Doppler-limited atomic absorption spectroscopy is inferred from the returned fluorescence intensity ratios at different frequencies.
- ❑ Both scanning and ratio techniques can work for the Doppler lidar. With scanning technique, the laser will be operated at many different frequencies, and then a least-square fit derives the width of the atomic absorption line, thus deriving the temperature. Its advantage is to provide more than 3 frequency information, so providing checks on more system parameters. But it requires longer integration time.
- ❑ Doppler ratio technique takes advantage of the high temporal resolution feature by limiting the lidar detection to 3 preset frequencies (usually one peak and two wing frequencies) for 3 unknown parameters (T , W , and density).
- ❑ By taking the ratios among signals at these three frequencies, R_T and R_W are sensitive functions of temperature and radial wind, respectively.



Summary (2)

- ❑ We compute the ratios R_T and R_W from atomic physics first to form the lidar calibration curves, and then look up the two ratios calculated from actual photon counts on the calibration curves to infer the corresponding temperature T and radial wind W.
- ❑ Different metrics exhibit different inhomogeneity, resulting in different crosstalk between T and W errors.
- ❑ There are several different atomic species (Na, K, Fe, Ca, Ca⁺, etc.) originating from meteor ablation in the mesosphere and lower thermosphere (MLT) region. They all have the potentials to be tracers for resonance fluorescence Doppler lidars to measure the temperature and wind in the MLT region.
- ❑ Na and K Doppler lidars are currently near mature status and making great contributions to MLT science.
- ❑ Fe Doppler lidar has very high future potential due to the high Fe abundance, advanced alexandrite laser technology, Doppler-free Fe spectroscopy, and bias-free measurements, etc.